Received 17 December 2023; revised 18 February 2024; accepted 3 March 2024. Date of publication 20 March 2024; date of current version 27 May 2024.

Digital Object Identifier 10.1109/OJAP.2024.3376514

Investigation of a Circularly Polarized Log-Periodic Dipole Antenna

KUNPENG WEI [1] (Senior Member, IEEE), XIAOPENG ZHANG [2], LIBIN SUN [3] (Member, IEEE), AND CHANGJIANG DENG [4,5] (Senior Member, IEEE)

[1]Mobile Phone Department, Xiaomi Communications Company Ltd., Beijing 100085, China

[2]Department of Electronic Engineering, Tsinghua University, Beijing 100084, China

[3]Consumer Business Group, Huawei Technologies Company Ltd., Shanghai 201206, China

[4]School of Integrated Circuits and Electronics, Beijing Institute of Technology, Beijing 100081, China

[5]Tangshan Research Institute, Beijing Institute of Technology, Tangshan 063099, China

CORRESPONDING AUTHOR: C. DENG (e-mail: dengcj11@bit.edu.cn)

This work was supported by the Beijing Natural Science Foundation-Xiaomi Innovation Joint Fund Project under Grant L233020.

ABSTRACT In this letter, a circularly-polarized (CP) log-periodic dipole antenna (LPDA) is investigated. Eight crossed dipole cells with a logarithmically increased λ/8 separation are employed to form the proposed CP LPDA. The dipoles with increased length and spacing are fed in series by an air-filled parallel line. The working mechanism of the generation of back-fire CP radiation is illustrated by an array analyzation. Besides, the LPDA design factors for both polarizations are analyzed in detail to realize an optimized CP performance. To validate the performance of the proposed eight-element CP LPDA, a prototype was fabricated and measured. The measured axial ratio (AR) bandwidth (0.8-2.5 GHz) is coincident with the impedance bandwidth (0.8-2.43 GHz), and it can be further increased with more elements. The overlapping bandwidth with VSWR < 2, AR < 3 dB, gain variation < 3 dB, and back-fire gain > 5 dBic is 0.94-2.43 GHz (2.6:1), and the radiation pattern is stable across the entire band.

INDEX TERMS Circularly-polarized (CP), frequency independent, log-periodic dipole antenna (LPDA), wideband.

I. INTRODUCTION

LOG-PERIODIC dipole antenna (LPDA) is a typical frequency-independent antenna, which has the merits of ultra-wideband, end-fire radiation, ease of fabrication, and light weight. The first LPDA is proposed by Isbell in [1], and later Carrel gives a detailed analysis and design guideline of LPDA in [2], [3]. However, the contours of computed gain versus σ and τ in [3] is incorrect, which leads to a higher gain. Then, the error is revised by Butson and Thompson [4] and an accurate optimized design guideline is proposed. In order to integrate with planar circuits, the printed planar LPDA is investigated in [5], [6]. Recently, many methods are investigated to reduce the overall size of LPDAs. In [7], [8], the arms of dipoles are bent multiple times to achieve Koch-shaped dipole. T-shaped top loading is also an effective method of reducing dipole and monopole size, which can also be integrated into LPDA [9], [10], [11]. Besides, dielectric loading [12] is also an effective means that can be combined with others. The antennas above are not suitable for mounting on metal platform. Because the profile will be very high when they are placed vertically. The miniaturized technique is also employed in [10], [11] to reduce the profile of LPDA when assembled on a metal platform. Therefore, they can be applied in aircrafts or vehicles to provide vertically polarized radiation.

The designs mentioned above are all linearly polarized (LP). Compared with LP antenna, circularly polarized (CP) antenna has some unique properties, such as combating the multi-path fading, reducing the Faraday rotation and polarization mismatch effect [13]. There are two basic ways to produce circular polarization (CP). One is that the element itself is circularly polarized, such as unequal length crossed dipole [14] and chamfered patch [15], etc. The other is to use the feeding circuit [16], [17], [18] to generate the phase difference required for CP. Many CP antennas in the form of line arrays have been studied. In [19] and [20], 45° tilted

© 2024 The Authors. This work is licensed under a Creative Commons Attribution-NonCommercial-NoDerivatives 4.0 License.
For more information, see https://creativecommons.org/licenses/by-nc-nd/4.0/

radiating elements are periodically added to both sides of the TEM transmission line. High gain broadside CP beam is obtained. Antennas with CP end-fire radiation are also designed in [21] and [22]. Each radiation element is capable of CP by itself. The end-fire radiation is achieved using a TEM transmission line. The bandwidth in [19], [20], [21], [22] is limited because the spacing of the radiating elements has to satisfy the required phase difference for broadside or end-fire radiation.

The CP line arrays based on LPDA have no bandwidth limiting factors other than dipole length ideally. The investigation of CP LPDA is limited and only a few researches has focused on the realization of CP LPDA [23], [24], [25]. In [23], a set of crossed dipoles with a distance logarithmically increased was proposed. Each crossed dipole cell contains two dipoles with different lengths to realize CP. The dipoles are fed by TEM transmission line. In [24] and [25], also unequal length crossed dipole is employed as the CP element of LPDA. However, the proposed CP element has a narrow AR bandwidth (ARBW).

Different from [23], [24], [25], crossed dipole with equal length is employed in the proposed CP LPDA. The CP radiation is achieved by separating the crossed dipoles with a distance of λ/8. Besides, an array analyzation is proposed to explain the working mechanism of the CP back-fire radiation. Then, the design difference for the two orthogonal polarizations is analyzed to reduce the gain difference between two polarizations and realize an optimized CP performance. The overlapping bandwidth of VSWR < 2, AR < 3 dB, gain variation < 3 dB, and back-fire gain > 5 dBic is 0.94-2.43 GHz (2.6:1).

II. ANTENNA DESIGN AND OPERATING MECHANISM

A. ANTENNA CONFIGURATION

The proposed antenna structure is depicted in Fig. 1 with eight crossed dipole cells, and the total length is 240 mm. Each cell includes two elements, a −45° polarized dipole (Dipole_1) and +45°polarized dipole (Dipole_2) [24]. The two dipoles in a cell are separated by a distance of S_i, which is about λ/8, to realize CP radiation in back-fire direction as shown in Fig. 1(a). The cells are logarithmically arranged to form the LPDA and the CP radiation will be enhanced. Besides, the lengths of the dipoles also increase logarithmically. Four types of dipoles are employed alternately in the array to realize desired phase reversal as shown in Fig. 1(b). The working mechanism of the array will be discussed in detail in Section II-B. An air-filled parallel line with width W_t and height H_t is utilized to excite all of the dipoles. The parallel line is fed through Port 1 by a coaxial cable. A 50 Ω matched load is connected to Port 2 to absorb the residual energy. The proposed antenna is an all-metal structure.

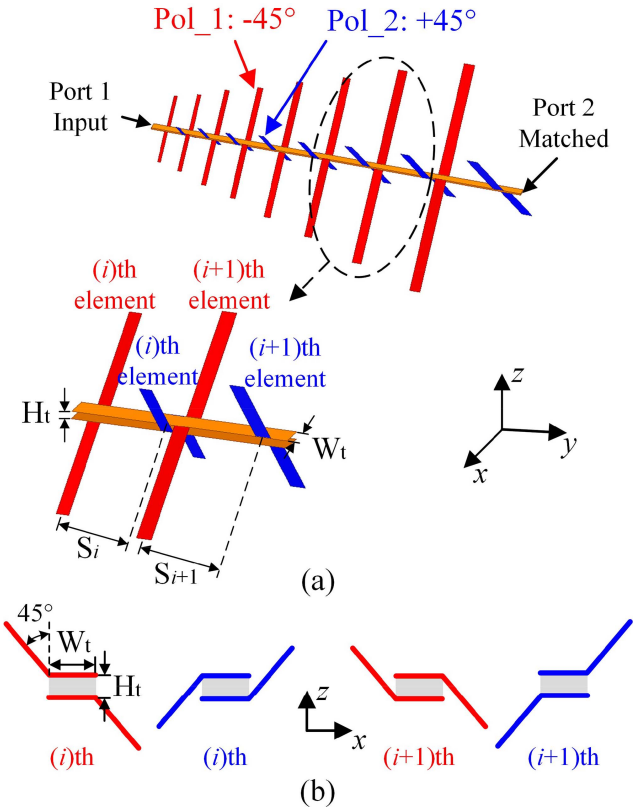

FIGURE 1. Configuration of the proposed CP LPDA. (a) 3D view, (b) side view of different dipole elements. Detailed dimensions: Wt = 5 mm, Ht = 1 mm.

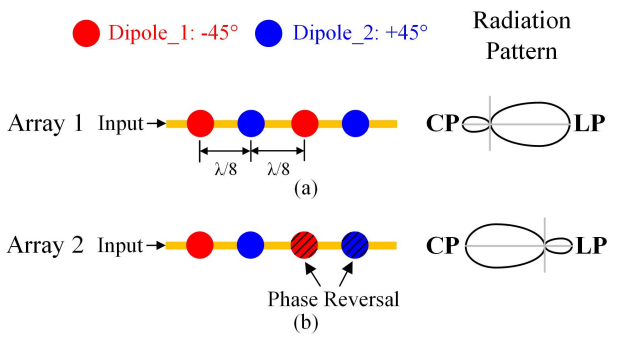

FIGURE 2. Array configurations of the series-fed crossed dipole cell. (a) The crossed dipole array with a distance of λ/8. (b) The crossed dipole array with a distance of λ/8 and phase reversal.

B. ARRAY CONFIGURATION OF THE SERIES-FED CROSSED DIPOLES

The working mechanism of the generation of CP radiation is analyzed in Fig. 2. Fig. 2 depicts two different array configurations of two crossed dipole cells. If the Dipole_1 element and Dipole_2 element are separated by λ/8, 90° and 0° phase shift will be achieved at the back-fire and end-fire directions, respectively. Because, in the back-fire direction, the 45° excited phase shift (λ/8) and 45° spatial phase shift (λ/8) between the Dipole_1 and Dipole_2 will be superimposed, while at the end-fire direction, the 45° excited phase shift and 45° spatial phase shift between the Dipole_1 and Dipole_2 will be cancelled out. Therefore, LP radiation in the end-fire direction and CP radiation in the back-fire direction will be realized respectively for Array 1. Besides, all of the elements are series fed by a transmission line with TEM mode, which makes the main beam point in the

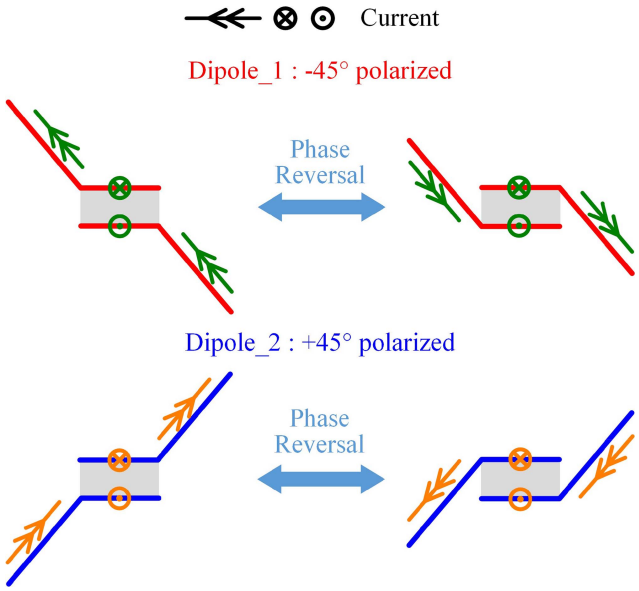

FIGURE 3. The mechanism of phase reversal for dipoles with same polarization.

end-fire direction as shown in Fig. 2(a). If we add a phase reversal for the second crossed dipole cell, the radiation pattern will be changed to a back-fire radiation. As a result, a CP back-fire radiation will be enhanced as presented in Array 2. Different from Array 1, the main beam of Array 2 points in the back-fire direction. A high gain CP radiation is obtained. Similarly, the dipoles in a cell should be separated with a distance of λ/8 to ensure a CP radiation in the back-fire direction.

In the proposed antenna, the phase reversal is achieved by employing different types of dipoles as shown in Fig. 1(b). The current of each dipole is illustrated in Fig. 3. Take the dipoles with −45° polarization as examples. The −45° polarization can be realized in two different ways. With the same current on the parallel line, the two different types of bending result in completely opposite currents on the dipoles according to the relative position. In other words, the two bending types make the dipoles with −45° polarization have currents with reverse phases. Similarly, the dipoles with +45° polarization have the same working mechanism. Based on these four basic dipoles in Fig. 3, the desired phase reversal is easily achieved. Moreover, the phase reversal can combine well with log-periodic alignment to further enhance the back-fire radiation.

C. ANALYZATION OF THE POL_1 AND POL_2 LPDAS

In Fig. 2, two adjacent cells are separated by a distance of λ/4 for back-fire radiation. However, the distance of λ/4 is not necessary in a log-periodic antenna. Back-fire radiation can be realized by adjusting spacing, dipole length and phase reversal together. From another perspective, the proposed CP LPDA in Fig. 1 can be divided into two LPDAs: Pol_1 and Pol_2 as shown in Fig. 4. The two arrays are composed of eight Dipole_1s and eight Dipole_2s, respectively. Either of them can realize backward LP radiation. Dipole_1s and

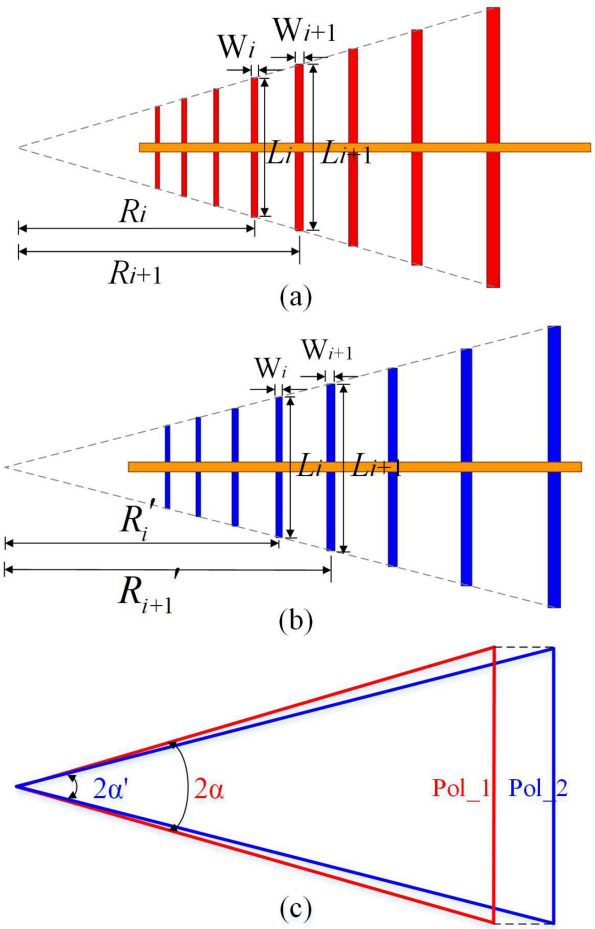

FIGURE 4. LPDAs for Pol_1 and Pol_2 and a comparison between them. (a) Pol_1 LPDA, (b) Pol_2 LPDA, (c) A comparison between the covered triangles formed by Pol_1 and Pol_2 LPDAs.

Dipole_2s used in these two arrays contain two types in Fig. 3, respectively, to realize the desired phase reversal of LPDA.

According to the analyzation in Section II-B, Pol_1 and Pol_2 should be separated by a distance of λ/8 to realize a CP radiation toward back-fire direction. Hence, the design factors are slightly different from each other as depicted in Fig. 4. The Pol_1 array shown in Fig. 4(a) is designed by the optimized curve in [27]. The detailed dimensions are proposed in Table 1 and the LPDA design factors are proposed in Table 2. Fig. 4(b) shows the Pol_2 array of the structure in Fig. 1. The lengths (L_i) and widths (W_i) of Pol_2 are equal with Pol_1. The simulated S_{11} of Pol_1 and Pol_2 is shown in Fig. 5. Both operate in the same frequency band. Compared with Pol_1, each dipole element in Pol_2 is moved backward with a distance S_i. In order to achieve 90° phase shift across the entire working bandwidth, the distance S_i is also increased logarithmically and satisfy:

$$\tau = \frac{S_i}{S_{i+1}} \tag{1}$$

The detailed dimensions of S_i are also shown in Table 1. As discussed in Section II-B, the distance S_i should be close

TABLE 1. Detailed dimensions (unit: mm).

Dipole element (i)	L_i	W_i	R_i	S_i
1	44	2	74.713	11
2	52.381	2.381	88.944	13.095
3	62.358	2.834	105.885	15.590
4	74.236	3.374	126.054	18.559
5	88.376	4.017	150.064	22.094
6	105.210	4.782	178.648	26.302
7	125.250	5.693	212.676	31.312
8	149.107	6.778	253.186	37.277

TABLE 2. LPDA design factors for Pol_1 and Pol_2.

	τ	σ	α
Pol_1	0.84	0.153	14.65°
Pol_2	0.84	0.156	12.84°

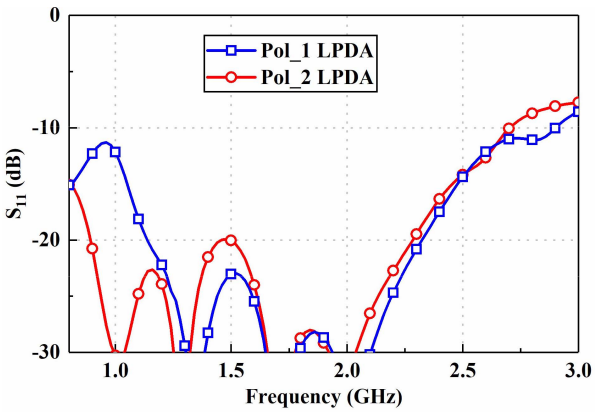

FIGURE 5. The simulated S_{11} of Pol_1 and Pol_2.

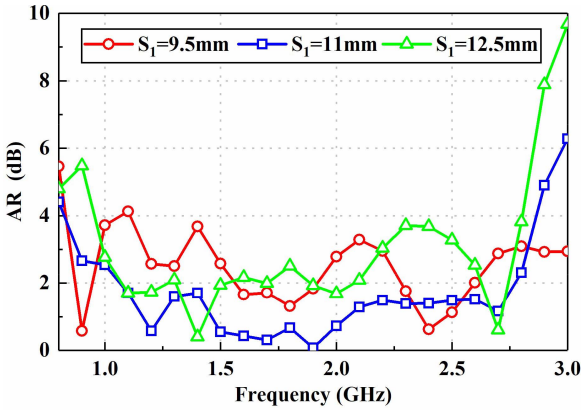

FIGURE 6. The simulate AR in back-fire direction versus S_1 with W_1 = 1mm.

TABLE 3. LPDA design factors.

	τ (τ')	σ	α	α'
LPDA1	0.8	0.153	18.10°	15.43°
LPDA2	0.84	0.153	14.65°	12.84°
LPDA3	0.88	0.153	11.10°	10.02°

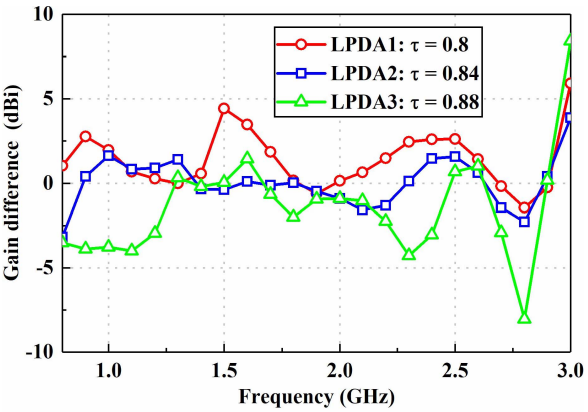

FIGURE 7. The gain difference (Gain(Pol_1) - Gain(Pol_2)) of three optimized LPDAs shown in Table 3 with different τ.

to λ/8. A longer or shorter value will significantly affect the CP performance. The effect of S_i on AR is shown in Fig. 6. As can be seen, when $S_1 = 11$ mm, AR less than 3 dB can be realized in a wide frequency band. The W_1 in Fig. 6 is 1 mm to avoid position conflicts of the arms.

The covered triangles for the Pol_1 and Pol_2 LPDAs are illustrated in Fig. 4(c). The angle α' of Pol_2 is slightly smaller than that of Pol_1 while the geometric ratio τ' of Pol_2 is equal with that of Pol_1. The relationship between α and α' can be deduced:

$$\tan\alpha' = \frac{L_i/2}{R'_i} = \frac{L_i/2}{R_i + S_i} = \frac{\tan\alpha}{1 + S_i/R_i} \tag{2}$$

Since the covered triangle of Pol_2 has a smaller slope and larger radiation aperture but doesn't satisfy the optimized curve. Thus, the gain of Pol_2 is different with that of Pol_1, which will deteriorate the CP performance. The difference between α and α' will be affected by the geometric ratio τ. Hence, it is a key step to optimize the geometric ratio τ to get a coincident gain between two polarizations. The design factors of three optimized LPDAs with different τ are shown in Table 3. The Gain difference (Gain(Pol_1) - Gain(Pol_2)) of these three optimized LPDAs are illustrated in Fig. 7. As can be seen, a least gain difference between two polarizations can be realized when $\tau = 0.84$. In this case, the gains of Pol_1 and Pol_2 are much closer over the entire frequency band, which mains that a stable gain of backward CP radiation can be realized.

D. CP AND E-FIELD

The simulated vector E-field distribution in a plane behind the proposed CP LPDA is shown in Fig. 8(a). As t increases from 0 to 3T/4, the direction of the electric vector rotates clockwise, which indicates that the proposed antenna is right-handed circular polarization (RHCP) in the -*y* direction. Fig. 8(b) illustrates the E-field distribution in *yz*-plane of the proposed antenna. It is obvious that the radiation is toward the back-fire direction.

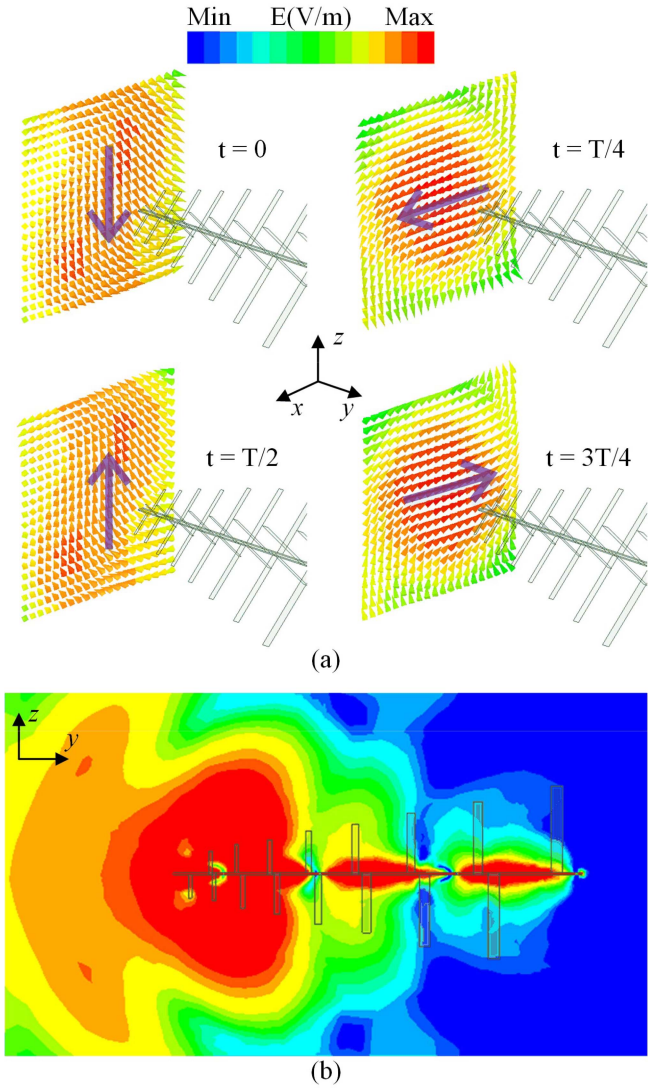

FIGURE 8. (a) The vector E-field distribution in a period at 2 GHz. (b) The magnitude E-field distribution in *yoz*-plane.

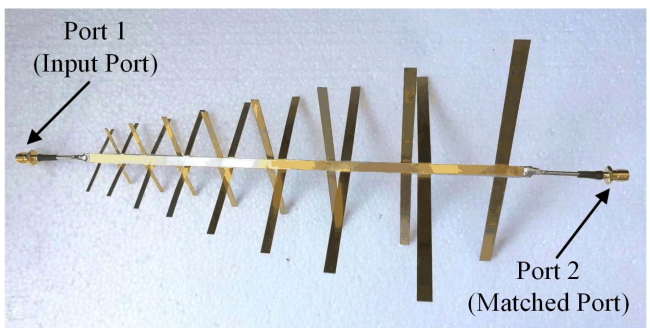

FIGURE 9. Photographs of the proposed antenna.

III. ANTENNA FABRICATION AND MEASUREMENT RESULTS

In order to validate the performance of the proposed CP LPDA, a prototype was fabricated as shown in Fig. 9. The LPDA is manufactured by a 0.5 mm thick copper plate, which is cut by the laser cutting technique with a precision of ±0.1 mm. The parallel line is filled with foam to ensure consistent height. The arms of the dipoles are manually bent to the right angle. Two 50-Ω semi-rigid cables are soldered at the two sides of parallel line. The excited signal is fed through Port 1, while Port 2 is connected with a matched load to absorb the residual energy.

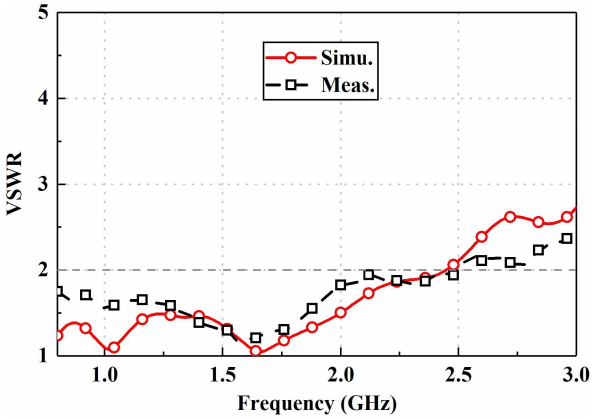

FIGURE 10. Simulated and measured VSWR.

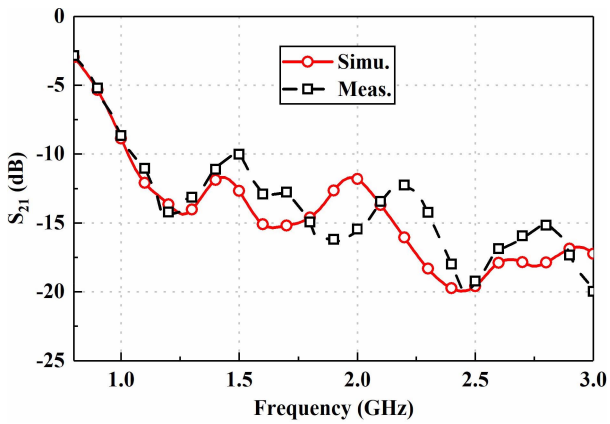

FIGURE 11. Simulated and measured S_{21}.

A. VSWR AND S_{21}

The VSWR of the proposed antenna is measured by a vector network analyzed (VNA), and the comparison curve between the simulated and measured results is shown in Fig. 10. The simulated bandwidth of VSWR < 2 is 0.8 - 2.45 GHz, while the measured bandwidth is 0.8 - 2.50 GHz. Since the radiation elements of the CP LPDA are doubled at a specified frequency, the leaky power is larger than that of the conventional LP LPDA. To estimate the leaky power, the simulated and measured S_{21} are shown in Fig. 11. At f < 0.9 GHz, the power is not radiated effectively but absorbed at the matched port. At f > 0.9 GHz and f < 3 GHz, a good power leaky of about 10–20 dB is realized. This means most of the energy is radiated into space.

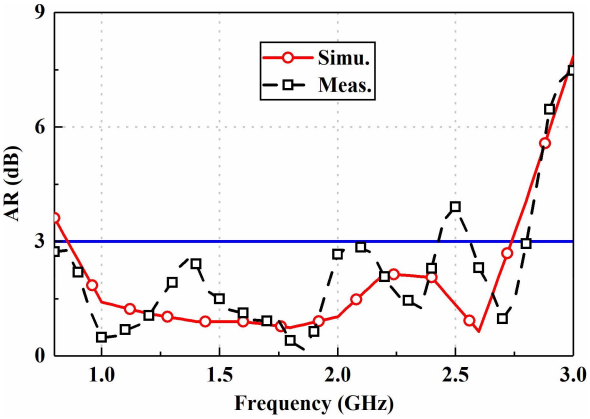

FIGURE 12. Simulated and measured AR.

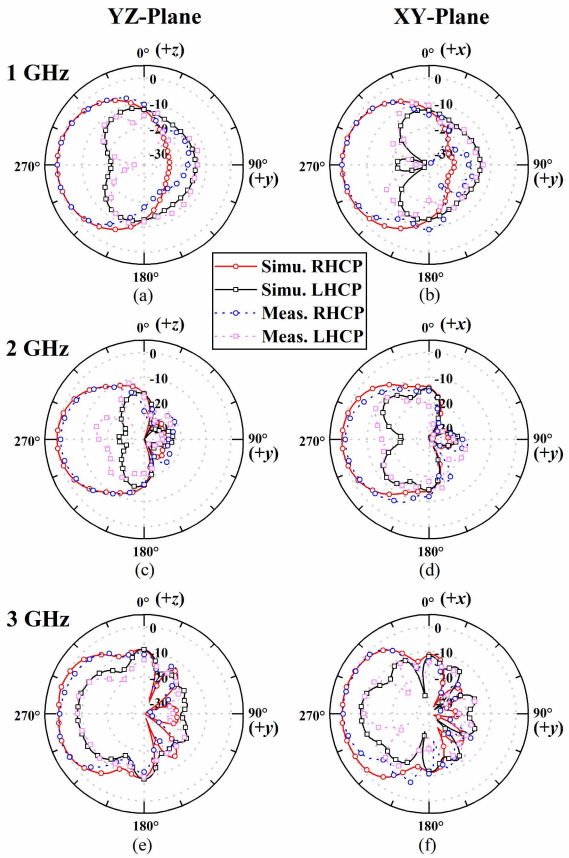

FIGURE 13. Simulated and measured normalized radiation pattern in two planes. (a) *yz*-plane at 1 GHz. (b) *xy*-plane at 1 GHz. (c) *yz*-plane at 2 GHz. (d) *xy*-plane at 2 GHz. (e) *yz*-plane at 3 GHz. (f) *xy*-plane at 3 GHz.

B. RADIATION PERFORMANCE

The simulated and measured AR in back-fire direction (-*y* direction) is shown in Fig. 12. The simulated 3 dB AR bandwidth is 0.85 - 2.68 GHz, while the measured 3 dB AR bandwidth is 0.8 - 2.43 GHz and 2.56-2.80 GHz. The measured AR at 2.43 - 2.56 GHz is deteriorated to 3 - 4 dB due to the fabrication deviation. The AR bandwidth is coincident with the impedance bandwidth, and the bandwidth can be further increased with more dipole elements.

The simulated and measured normalized radiation patterns at 1, 2, and 3 GHz in two planes are shown in Fig. 13. A stable back-fire radiation pattern can be realized across the entire band. The measured and simulated RHCP patterns coincide well with each other. The cross-polarization levels are low in -*y* direction at 1 and 2 GHz because of the low AR levels. The curve of back-fire gain versus frequency is shown in Fig. 14. Small deviation is occurred between the simulated and measured results due to the fabrication error. The measured maximum gain is 8.15 dBic, and the gain is stable with variation less than 3 dB across 0.94 - 3 GHz.

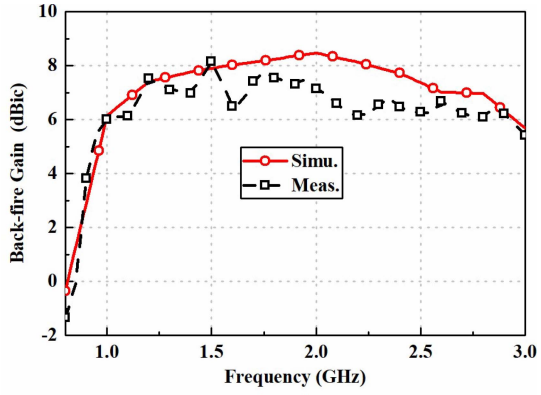

FIGURE 14. Simulated and measured back-fire gain.

TABLE 4. Comparisons of CP antennas.

Ref.	Crossd dipole	Size(λ_0^3)	Impedance BW(GHz)	AR BW	Peak gain (dBic)
[17]	Equal	0.38×0.9 ×0.9	1.9 – 4.4 (1.3:1)	65%	9.7
[18]	Equal	0.25×1.0 3×1.03	3.16-6.34 (1:1)	53%	10.62
[23]	Unequal	0.86×0.3 8×0.43	0.85 - 2.16 (2.5:1)	50%	5.31
[24]	Unequal	0.75×0.5 5×0.64	3.3 - 5.7 (1.7:1)	≈100%	6.5
Ours	Equal	1.35×0.8 3×0.82	0.94 - 2.43 (2.6:1)	100%	8.15

C. DISCUSSION

The comparisons between the proposed antenna and previous CP antennas are reported in Table 4. In [17] and [18], two cavity-backed crossed dipole antennas are proposed. Compared with single antenna, our proposed array has significant advantages in both impedance bandwidth and ARBW. Because our design based on log-periodic arrangement allows different lengths of crossed dipoles to be operated at different frequencies. The gain is slightly lower. This is because our proposed antenna does not utilize a large metal reflector. In [23] and [24], the antennas are designed based on unequal length crossed dipole. Differently, our proposed antenna is designed based on equal length crossed dipole. The CP is achieved by adjusting the feeding and

spatial phase difference and the phase reversal. Compared to these two designs, the proposed antenna achieves a wider relative impedance bandwidth. And the ARBW is also very wide. The peak gain is benefited from the larger size to some extent. It is worth mentioning that the size reduction methods in [23] and [24] can be applied to our proposed antenna to reduce the size.

IV. CONCLUSION

This article proposes a detailed investigation of CP LPDA. The wideband CP LPDA is realized by a logarithmically increased $\lambda/8$ separation between $+45°$ polarized and $-45°$ polarized LPDAs. Therefore, an overlapping bandwidth of 0.94-2.43 GHz (2.6:1) with VSWR<2, AR < 3 dB, gain variation < 3 dB, back-fire gain >5 dBic is realized. Furthermore, the overlapping bandwidth can be further increased with more elements, the frequency-independent property is still satisfied in the proposed CP LPDA.

REFERENCES

[1] D. E. Isbell, "Log periodic dipole arrays," *IRE Trans. Antennas Propag.*, vol. 8, no. 3, pp. 260–267, May 1960.

[2] R. Carrel, "The design of log-periodic dipole antennas," in *Proc. IRE Int. Conv. Rec.*, vol. 9, 1961, pp. 61–75.

[3] R. Carrel, "Analysis and design of the log-periodic dipole antenna," Ph.D. Dissertation, Dept. Electr. Eng., University of Illinois, Champaign, IL, USA, 1961.

[4] P. Butson and G. Thompson, "A note on the calculation of the gain of log-periodic dipole antennas," *IEEE Trans. Antennas Propag.*, vol. 24, no. 1, pp. 105–106, Jan. 1976.

[5] C. K. Campbell, I. Traboulay, M. S. Suthers, and H. Kneve, "Design of a stripline log-periodic dipole antenna," *IEEE Trans. Antennas Propag.*, vol. 25, no. 5, pp. 718–721, Sep. 1977.

[6] R. R. Pantoja, A. R. Sapienza, and F. C. M. Filho, "A microwave printed log-periodic dipole array antenna," *IEEE Trans. Antennas Propag.*, vol. 35, no. 10, pp. 1176–1178, Oct. 1987.

[7] D. E. Anagnostou, J. Papapolymerou, M. M. Tentzeris, and C. G. Christodoulou, "A printed log-periodic Koch-dipole array (LPKDA)," *IEEE Antennas Wireless Propag. Lett.*, vol. 7, pp. 456–460, 2008.

[8] H. T. Hsu and T. J. Huang, "A Koch-shaped log-periodic dipole array (LPDA) antenna for universal ultra-high-frequency (UHF) radio frequency identification (RFID) handheld reader," *IEEE Trans. Antennas Propag.*, vol. 61, no. 9, pp. 4852–4856, Sep. 2013.

[9] J. Chen, J. Ludwig, and S. Lim, "Design of a compact log-periodic dipole array using T-shaped top loading," *IEEE Antennas Wireless Propag. Lett.*, vol. 16, pp. 1585–1588, 2017.

[10] Z. Hu, Z. Shen, W. Wu, and J. Lu, "Low-profile log-periodic monopole array," *IEEE Trans. Antennas Propag.*, vol. 63, no. 12, pp. 5484–5491, Dec. 2015.

[11] Q. Chen, Z. Hu, Z. Shen, and W. Wu, "2–18 GHz conformal low-profile log-periodic array on a cylindrical conductor," *IEEE Trans. Antennas Propag.*, vol. 66, no. 2, pp. 729–736, Feb. 2018.

[12] L. Chang, S. He, J. Q. Zhang, and D. Li, "A compact dielectric-loaded log-periodic dipole array (LPDA) antenna," *IEEE Antennas Wireless Propag. Lett.*, vol. 16, pp. 2759–2762, 2017.

[13] S. Gao, Q. Luo, and F. Zhu, *Circularly Polarized Antenna*. Hoboken, NJ, USA: Wiley, 2014.

[14] L.-K. Zhang, Y.-X. Wang, J.-Y. Li, Y. Feng, and W. Zhang, "Cavity-backed circularly polarized cross-dipole phased arrays," *IEEE Antennas Wireless Propag Lett.*, vol. 20, pp. 1656–1660, 2021.

[15] K. Y. Lam, K.-M. Luk, K. F. Lee, H. Wong, and K. B. Ng, "Small circularly polarized U-slot wideband patch antenna," *IEEE Antennas Wireless Propag. Lett.*, vol. 10, pp. 87–90, 2011.

[16] Y. Zhang, Y. Li, M. Hu, P. Wu, and H. Wang, "Dual-band circular-polarized microstrip antenna for ultrawideband positioning in smartphones with flexible liquid crystal polymer process," *IEEE Trans. Antennas Propag.*, vol. 71, no. 4, pp. 3155–3162, Apr. 2023.

[17] T. K. Nguyen, H. H. Tran, and N. Nguyen-Trong, "A wideband dual-cavity-backed circularly polarized crossed dipole antenna," *IEEE Antennas Wireless Propag. Lett.*, vol. 16, pp. 3135–3138, 2017.

[18] G. Feng, L. Chen, X. Xue, and X. Shi, "Broadband circularly polarized crossed-dipole antenna with a single asymmetrical cross-loop," *IEEE Antennas Wireless Propag. Lett.*, vol. 16, pp. 3184–3187, 2017.

[19] T. R. Cameron, A. T. Sutinjo, and M. Okoniewski, "A circularly polarized broadside radiating 'herringbone' array design with the leaky-wave approach," *IEEE Antennas Wireless Propag Lett.*, vol. 9, pp. 826–829, 2010.

[20] G. Mishra, S. K. Sharma, and J.-C. S. Chieh, "A high gain series-fed circularly polarized traveling-wave antenna at W-band using a new butterfly radiating element," *IEEE Trans. Antennas Propag.*, vol. 68, no. 12, pp. 7947–7957, Dec. 2020.

[21] Z. Wu, Z. Miao, R. Gao, and L. Xiao, "Series-fed all-metal and wide-axial-ratio-bandwidth circularly polarized leaky-wave antenna with endfire radiation," *IEEE Antennas Wireless Propag. Lett.*, vol. 21, pp. 646–650, 2022.

[22] Z. Wu, Z. Miao, and X. Deng, "High-gain and wideband circularly polarized endfire leaky-wave antenna array based on the complementary dipole," *IEEE Trans. Antennas Propag.*, vol. 71, no. 7, pp. 6168–6172, Jul. 2023.

[23] K. A. Leon, J. Haney, and S. Lim, "A size-reduced, circularly polarized, log-periodic dipole array," *IEEE Antennas Wireless Propag. Lett.*, vol. 21, pp. 371–375, 2022.

[24] G. Liu, L. Xu, and Z. Wu, "Miniaturised wideband circularly-polarized log-periodic Koch fractal antenna," *Electron. Lett.*, vol. 49, no. 21, pp. 1315–1316, Oct. 2013.

[25] J. Haney and S. Lim, "A miniaturized, circularly polarized log periodic dipole array," in *Proc. Int. Workshop. Antenna Technol. (iWAT)*, 2016, pp. 80–81.

[26] K. Wei, Z. Zhang, Z. Feng, and M. F. Iskander, "Periodic leaky-wave antenna array with horizontally polarized omnidirectional pattern," *IEEE Trans. Antennas Propag.*, vol. 60, no. 7, pp. 3165–3173, Jul. 2012.

[27] C. A. Balanis, *Antenna Theory Analysis and Design*, 3rd ed. Hoboken, NJ, USA: Wiley, 2005.

KUNPENG WEI (Senior Member, IEEE) received the B.S. degree in electronic and information engineering from the Huazhong University of Science and Technology, Wuhan, China, in 2008 and the Ph.D. degree in electrical engineering from Tsinghua University, Beijing, China, in 2013.

From July 2013 to December 2015, he was employed with the Radar Research Institute of Chinese Air Force Research Laboratory, conducting research in the areas of phased-array antenna design and radar system design. He joined the Consume Business Group of Huawei Inc. in 2016, where he had been an Antenna Specialist and the Director of Xi'an Antenna Team for five years. In 2021, he joined Honor Device Company Ltd. when this company split from Huawei and he was the Director of Honor Antenna Team. After leaving Honor, he joined Xiaomi Corporation, Beijing, in 2023. He is currently the Chief Antenna Expert and the Head of the Antenna Technology Team. He leads a large group of antenna experts and engineers, and takes the full responsibility in the research of antenna technologies to guarantee the market success of all Xiaomi's products ranging from smartphones, electric cars, tablets, laptops, and other IOT devices. He is also a special level External Expert of the China Academy of Information and Communications Technology. He is also an Adjunct Professor with the School of Electronics and information engineering, Shenzhen University, China. He has authored over referred 50 papers on consumer electronics antenna design. He holds over 50 granted U.S./EU/JP/CN patents and has other 20+ patent applications in pending. His current research interests include meta-antennas, smart-phone antenna design, small size 5G antenna systems in terminal device, and millimeter-wave antenna array.

Dr. Wei was a recipient of the Principal Scholarship of Tsinghua University in 2012, the Huawei Individual Gold Medal Award in 2018, the Huawei Team Gold Medal Award in 2017, and the Honor Team Gold Medal Award in 2021, respectively. He has been serving as an Associate Editor for IET ELECTRONICS LETTERS since October 2021 and IEEE OPEN JOURNAL OF ANTENNAS AND PROPAGATION since October 2023. He is an IET Fellow.

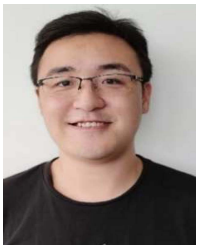

XIAOPENG ZHANG received the B.S. degree from Xidian University, Xi'an, China, in 2019. He is currently pursuing the Ph.D. degree with the Department of Electrical and Engineering, Tsinghua University, Beijing, China. His current research interests include leaky-wave antennas, antenna decoupling, and MIMO.

LIBIN SUN (Member, IEEE) received the B.S. degree from Xidian University, Xi'an, China, in 2016, and the Ph.D. degree in electronic engineering from Tsinghua University, Beijing, China, in 2021.

He is currently working with the Consumer Business Group, Huawei Technologies Company Ltd., Shanghai, as a Senior Antenna Engineer. He has authored or coauthored over 15 journal papers and holds five granted Chinese patents. His current research interests include antenna design and electromagnetic theory, particularly in 5G mobile phone antennas, antenna decoupling techniques and MIMO antennas, millimeter-wave antennas, and interaction effects between antenna and human body.

Dr. Sun was a recipient of the Top Reviewer Award for the IEEE Transactions on Antennas and Propagation in 2019, the Honorable Mention in 2020 IEEE AP-S Student Paper Competition, the Chinese National Doctorial Scholarship in 2019, and the Principal Scholarship (Highest Honor) of Tsinghua University in 2020. He has served as the Session Chair for the APMC 2020 and serves as a reviewer for several international academic journals, such as the IEEE TRANSACTIONS ON ANTENNAS AND PROPAGATION, IEEE ANTENNAS AND WIRELESS PROPAGATION LETTERS, IEEE ACCESS, *IET Microwaves, Antennas and Propagation*, *IET Electronics Letters*, and *Microwave and Optical Technology Letters*.

CHANGJIANG DENG (Senior Member, IEEE) received the B.S. degree in communication engineering from Beijing University of Posts and Telecommunications, Beijing, China, in 2011, and the Ph.D. degree in electrical engineering from Tsinghua University, Beijing, in 2016.

He was a Visiting Scholar with the Radiation Laboratory, University of Michigan from 2018 to 2019. He is currently an Associate Professor with School of Integrated Circuits and Electronics, Beijing Institute of Technology, Beijing, where he is with the Beijing Key Laboratory of Millimeter Wave and Terahertz Technology, School of Integrated Circuits and Electronics. He is also with the Tangshan Research Institute, Beijing Institute of Technology, Tangshan, China. His research interests include mobile phone antennas, MIMO antennas, phased array antennas, and reconfigurable intelligence surface. He received the EMTS Young Scientist Award from URSI Commission B in 2019. He is an Associate Editor of *IET Microwaves, Antennas and Propagation*. He also serves as a reviewer for several journals, including *Nature Communication* and IEEE TRANSACTIONS ON ANTENNAS AND PROPAGATION.